Journal of Power Sources 220 (2012) 31–41

Contents lists available at SciVerse ScienceDirect

Journal of Power Sources

journal homepage: www.elsevier.com/locate/jpowsour

Proton exchange membrane fuel cells cold startup global strategy for fuel cell plug-in hybrid electric vehicle

Nilson Henao [a], Sousso Kelouwani [b,*], Kodjo Agbossou [a], Yves Dubé [b]

[a] Hydrogen Research Institute and the Department of Electrical and Computer Engineering of Université du Québec à Trois-Rivières, Trois-Rivières, Québec G9A 5H7, Canada
[b] Hydrogen Research Institute and the Department of Mechanical Engineering of Université du Québec à Trois-Rivières, Trois-Rivières, Québec G9A 5H7, Canada

HIGHLIGHTS

- The design and the experimental validation of a supervisory architecture for FC-PHEV energy management.
- The design of a global strategy for the fuel cell cold startup.
- A time optimal heating method based on the Pontryagin minimum principle.

ARTICLE INFO

Article history:
Received 23 May 2012
Received in revised form
28 July 2012
Accepted 30 July 2012
Available online 7 August 2012

Keywords:
Electric vehicles
Energy efficiency
Energy management
Fuel cells cold startup
Nonlinear optimal control
Vehicle dynamics

ABSTRACT

This paper investigates the Proton Exchange Membrane Fuel Cell (PEMFC) Cold Startup problem within the specific context of the Plugin Hybrid Electric Vehicles (PHEV). A global strategy which aims at providing an efficient method to minimize the energy consumption during the startup of a PEMFC is proposed. The overall control system is based on a supervisory architecture in which the Energy Management System (EMS) plays the role of the power flow supervisor. The EMS estimates in advance, the time to start the fuel cell (FC) based upon the battery energy usage during the trip. Given this estimation and the amount of additional energy required, the fuel cell temperature management strategy computes the most appropriate time to start heating the stack in order to reduce heat loss through the natural convection. As the cell temperature rises, the PEMFC is started and the reaction heat is used as a self-heating power source to further increase the stack temperature. A time optimal self-heating approach based on the Pontryagin minimum principle is proposed and tested. The experimental results have shown that the proposed approach is efficient and can be implemented in real-time on FC-PHEVs.

1. Introduction

The hydrogen fuel cell is emerging as one of the best power sources for the sustainable transportation due to its low greenhouse gas emission and its high power density [1,2]. Different types of fuel cell technologies are being investigated for Hybrid Electric Vehicle (HEV). However, the Proton Exchange Membrane Fuel Cell (PEMFC) is one of the most selected power sources for electric mobility [3]. In some vehicle applications involving fuel cells, the batteries are being used primarily to capture the regenerative power, secondary to absorb the rapid and high power transient originating from the vehicle dynamics and finally to provide power to the vehicle motion [4]. These vehicles are designated as Fuel Cell Plug-in Hybrid Electric Vehicle (FC-PHEV). The energy efficiency of an FC-PHEV is thoroughly related to the power flow management between all components that contribute to the vehicle propulsion. So, a lot of work is being done on the specific problem of the on-board energy management and power splitting [5].

When the fuel cell is operating, there is a production of water and water vapor. Although a systematic purge is performed during the PEMFC shutdown process, the remaining water vapor could frost when the temperature drops below 0 °C (in regions with long and very cold winter seasons). To preserve the fuel cell life, a specific attention is required before restarting the fuel cell during the periods of sub-freezing and freezing ambient temperatures [6–8]. Thus, Ref. [9] reported that an irreversible degradation in the fuel cell components occurs during sub-freezing and freezing operating temperatures. The volume expansion of the cell materials in the freezing conditions is one of the reasons for this degradation

* Corresponding author. Tel.: +1 819 376 5011; fax: +1 819 376 5210.
E-mail addresses: Nilson.Henao@uqtr.ca (N. Henao), sousso.kelouwani@uqtr.ca (S. Kelouwani), kodjo.agbossou@uqtr.ca (K. Agbossou), yves.dube@uqtr.ca (Y. Dubé).

0378-7753/$ – see front matter © 2012 Elsevier B.V. All rights reserved.
http://dx.doi.org/10.1016/j.jpowsour.2012.07.088

[10]. Among the proposed recommendations in Refs. [9,10] is the water purge operation during the fuel cell shutdown. The research reported in Refs. [11,12] showed that heating the stack has a great positive impact on the fuel cell transient thermal model. In Ref. [13], the catalytic oxygen/hydrogen reaction heat is used to increase the stack temperature.

In physics and in electrochemistry, several studies regarding the stack self-heating when the stack temperature belongs to a sub-freezing range, have been reported. The cell membrane water content and the ice formation in the cathode catalyst layer are extensively studied and identified as the main performance limiting factors. In Ref. [21], an analytical model describing the heat balance, the ice formation in the catalyst layer, and the water transport characteristic throughout a fuel cell at very low temperatures is presented. In Ref. [22], numerical studies were conducted using a monotonically increasing current for a fuel cell cold start from −30 °C. It was shown that using a moderate current increasing rate or using a large initial current density in combination with a small current increasing rate, can lead to a successful stack self-start. In the experimental study presented in Ref. [23], the ice accumulation in a frozen PEMFC was measured at sub-freezing temperatures and the time to voltage failure for various current densities under isothermal operation at −20 °C was also measured.

Although these reported studies demonstrated that it is possible to achieve a fuel cell self-start from a sub-freezing temperature, we propose in this paper a different approach which focuses only on the stack thermodynamic and electric aspects. This approach allows us to consider the PEMFC global electrothermal behavior without focusing on the electrochemistry detail equations. In addition, the electrothermal behavior model permits a simple and effective formulation of the global optimization problem that can be solved in real-time in the context of the FC-PHEV. To avoid complicated water management issues and potential irreversible damages in the fuel cell components, an external heating system is used to heat the stack and let the cell temperature to belong to its normal operating range from a sub-freezing starting point.

Two different methods have been reported for the fuel cell heating [7]. The internal heating which is the first method, consists in providing an electric current to a resistance embedded directly into the stack. The heat generated from the resistance Joule effect is transferred to the stack structure. Often, this method is used by the fuel cell manufacturers. The second method is related to the external fluid based warm-up system which uses a heat exchanger and an antifreeze fluid (mixture of glycol and water). The exchanger allows the heat transfer from the fluid to the stack components. This method is more accessible to our research than the previous one. However, the main problem is to determine the heating energy (heating power and duration) that will allow rising the stack temperature whilst minimizing the heat loss through the natural convection with the environment.

This paper investigates the PEMFC temperature management for the vehicle application, especially for the FC-PHEV vehicles. On such a vehicle, the batteries have the energy to propel the vehicle over a portion of the travel distance and the fuel cell, which plays the role of range extender, is started to recharge the batteries through a serial topology [14].

We assume that the fuel cell has an appropriate heat exchanger embedded into the cells to allow the warm-up process using an external fluid heating system. Two contributions are presented: the first one is related to the design and to the experimental validation of a two layer supervisory architecture for FC-PHEV energy management. The second contribution consists in designing a global strategy for the fuel cold startup by considering the cells initial temperature, the ambient temperature, the thermal operating range of the cells and the amount of energy available for heating the stack. The vehicle Energy Management System (EMS) is part of the upper layer whereas the global strategy for the fuel cell cold startup belongs to the lower layer. Knowing the trip length and the average power requirement for the vehicle motion, this EMS estimates the amount of fuel cell energy required to complete the trip. It also estimates in advance the appropriate time to start the fuel cell. The global strategy for the fuel cell cold startup uses these two data as constraints and provides the appropriate heating timing that will allow the fuel cell to comply with them.

The rest of the paper is organized in 7 sections. The FC-PHEV supervisory architecture is presented in section 2. The cold start problem overview and the startup strategy are discussed in sections 3 and 4, respectively. The self-heating method based on the Pontryagin minimum principle is investigated in section 5, whereas the high temperature regulation and the experimental results are discussed in sections 6 and 7, respectively. Finally the conclusion is presented in section 8.

2. FC-PHEV supervisory architecture

Fig. 1 represents a typical FC-PHEV serial topology where the solid and dashed arrows represent the power flow and the control signal, respectively. The driver power demand is sent to the Energy Management System (EMS) which generated the corresponding power command P_m for Electric Propulsion System. The bi-directional converter allows the Battery Pack to be charged and discharged and P_b represents the power flowing through this converter. In this architecture the EMS supervises the Fuel Cell Power Controller and the battery pack energy E_b. The power from the Fuel Cell P_{fc} is used to recharge the batteries.

To prevent the Battery Pack to be over discharged, a minimum energy threshold E_b^{min} is usually defined [15]. So the Battery Pack is operating in a depleting mode until E_b reaches E_b^{min}. Knowing the initial Battery Pack energy E_b^0, the amount of energy available for the trip and the stack heating is represented by:

$$E_b^a = E_b^0 - E_b^{min} - E_{he}^{max} \quad (1)$$

where E_{he}^{max} is the maximum energy that can be used to heat the stack.

We assume that the whole trip duration t_{td} and the average traction power $\tilde{P}_m$ are known; thus, it is possible to approximate the total energy required to drive the vehicle to the destination using the following equation:

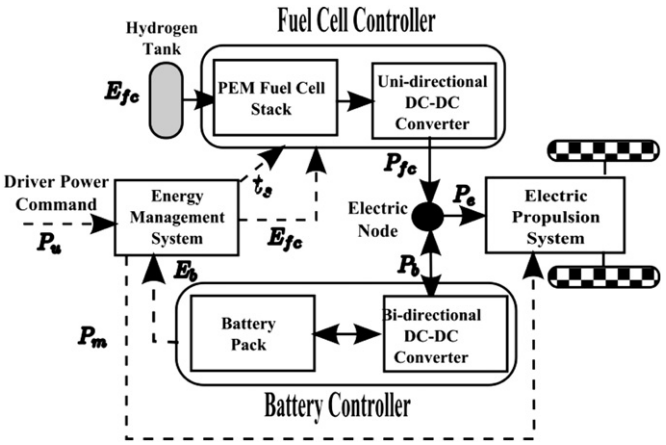

Fig. 1. Fuel cell hybrid electric Vehicle: the arrows with solid lines represent energy flows; the arrows with dashed lines represent control and measured signals.

$$\tilde{E}_{tr} = \tilde{P}_m t_{td} \quad (2)$$

If $(E_b^a < \tilde{E}_{tr})$, the additional energy required for the Fuel Cell is therefore estimated using the following equation:

$$\tilde{E}_{fc} = \tilde{E}_{tr} - E_b^a \quad (3)$$

As the battery energy E_b reaches E_b^{min}, the fuel cell is started to recharge batteries. Since the fuel cell needs to be warm-up before being started, the EMS must anticipate when the batteries minimum energy E_b^{min} will be attained. If P_m is perfectly predictable, then the time t_{st} to reach E_b^{min} is obtained by solving the following equation:

$$E_b^0 - \int_0^{t_{st}} P_m(t)dt - E_{he}^{max} = E_b^{min} \quad (4)$$

where E_b^0 is the Battery pack initial energy and where $t_{st} \geq 0$.

In practice, the perfect knowledge of P_m which depends on the value of P_u is difficult to obtain because the vehicle driver command is related to the unpredictable factors such as the traffic, the road conditions, etc. So, an approximation $\tilde{t}_{st}$ of t_{st} is required.

2.1. Estimation of t_{st}

Assume that at time $t < t_{st}$, the past values of $P_m(t)$ are known. So the time to reach E_b^{min} is given by:

$$E_b^0 - \int_0^t P_m(\tau)d\tau - \int_t^{\tilde{t}_{st}} \tilde{P}_m(\tau)d\tau - E_{he}^{max} = E_b^{min} \quad (5)$$

Since $\tilde{P}_m$ is the average power obtained with the past values of P_m, Eq. (5) becomes:

$$E_b^0 - \int_0^t P_m(\tau)d\tau - \tilde{P}_m(\tilde{t}_{st} - t) - E_{he}^{max} = E_b^{min} \quad (6)$$

Hence, $\tilde{t}_{st}$ is obtained using the following equation:

$$\tilde{t}_{st} = t + \frac{E_b^0 - \int_0^t P_m(\tau)d\tau - E_b^{min} - E_{he}^{max}}{\tilde{P}_m} \quad (7)$$

3. Cold start problem overview

The target of the cold startup strategy is related to the Hybrid Electrical Vehicles (HEVs) with a PEMFC as a range extender power source. We assume that the vehicle EMS provides the estimated startup time $\tilde{t}_{st}$ and the estimated fuel cell energy production $\tilde{E}_{fc}$. Furthermore, we assume that the initial temperature T_{fc}^0 of the PEMFC as well as the ambient temperature T_{amb} are also known beforehand. If T_{fc}^0 and T_{amb} are in the sub-freezing temperature range, it is recommended to warm-up the fuel cell above the freezing temperature in order to avoid complex fluid management issues, ice build-up and to preserve the cell's life [9,10].

Indeed, the PEMFC have an operating temperature range $(T_{fc}^{min} \leq T_{fc} \leq T_{fc}^{max})$ which depends on the type of technology and the factory specifications. Since the amount of energy required to warm-up the fuel cell is limited to E_{he}^{max}, the first problem to solve is to determine the appropriate time to start the fuel cell warm-up system in order to minimize the heat transfer from the fuel cell structure to the environment. The operation of this system will help the stack temperature to increase from its sub-freezing point to the T_{fc}^{min}.

As the stack temperature T_{fc} reaches T_{fc}^{min}, the fuel cell can be started safely. The electrochemical model of the PEMFC shows that the efficiency is related to several parameters such as the temperature, the air humidity ratio and the air stoichiometry. Since we are mainly interested in the temperature effect on the PEMFC work point, several studies and analyses have demonstrated that by increasing the temperature, the fuel cell efficiency is improved for high power production [24,25].

When T_{fc} reaches T_{fc}^{min}, it is not efficient to use the battery energy to heat the fuel cells in order to raise its temperature quickly. Instead, the heat from the exothermic reaction in the fuel cell is used to increase the stack temperature. The second problem is to find an optimal fuel cell power production profile in order to increase as quickly as possible the stack temperature without exceeding the prescribed maximum temperature T_{fc}^{max}.

When the stack temperature reaches T_{fc}^{max}, a cooling process must be started to prevent overheating cells. The PEMFC high temperature regulation has been solved in the literature and numerous methods have been proposed. Therefore, it will not be analyzed in this paper.

4. Cold startup strategy

4.1. Stack warm-up strategy

In this section we propose a method that will provide the most appropriate time $t_{st,he}$ to start the warm-up system to increase the fuel cell stack temperature using the following assumptions:

- the time to start the PEMFC $\tilde{t}_{st}$ is given by the EMS;
- the amount of energy to produce is also given;
- the heating fluid is incompressible;
- the PEMFC model is represented by the heating thermal mass m_{fc} and the average specific heat capacity c_{fc};
- he heating power of the warm-up system is fixed and known beforehand.

Fig. 2 represents the warm-up system connected to the PEMFC stack.

The first order heat transfer model of the system is represented by the following system of differential linear equations:

$$\begin{cases} m_w c_w \dot{T}_w = P_{he} - \dot{Q}_{whe} \\ m_{fc} c_{fc} \dot{T}_{fc} = -\dot{Q}_{amb} + \dot{Q}_{whe} \end{cases} \quad (8)$$

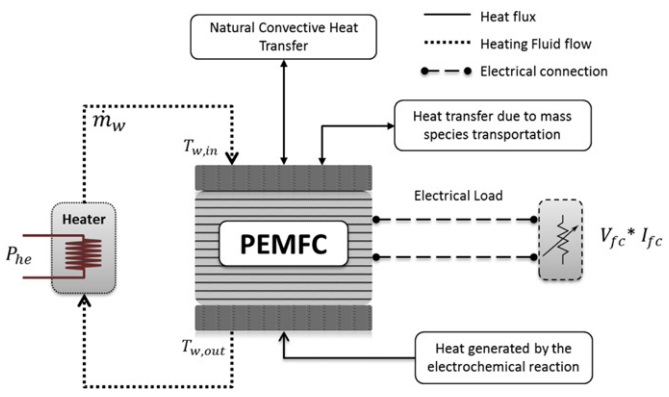

Fig. 2. Warm-up system and PEMFC.

where m_w, m_{fc}, c_w, c_{fc}, T_w, P_{he}, $\dot{Q}_{amp}$, and $\dot{Q}_{whe}$ represent the heating fluid mass, the stack mass, the average specific heat coefficient of the heating fluid, the average specific heat coefficient of the fuel cell, the heating fluid average temperature, the heating element power, the stack-environment heat transfer rate (see Eq. (9)) and the heating element heat transfer rate (see Eq. (10)), respectively.

$$\dot{Q}_{amb} = h_{nc}S_{nc}\left(T_{fc} - T_{amb}\right) \tag{9}$$

where h_{nc}, S_{nc}, T_{amp} and T_{fc} represent the natural convective heat transfer coefficient, the effective heat transfer surface (between the stack and the environment), the ambient temperature and the fuel cell temperature, respectively.

In the considered open thermodynamic system, the heat transferred by the heating fluid is represented by:

$$\dot{Q}_{whe} = \dot{m}_w c_w \left(T_{w,out} - T_{w,in}\right) \tag{10}$$

where $\dot{m}_w$, $T_{w,in}$ and $T_{w,out}$ represent the heating fluid mass flow rate, the temperatures of the heating fluid that is entering and exiting the stack, respectively.

The expression for the outlet fluid temperature is given by [20]:

$$T_{w,out} = T_{fc} + \left(T_{w,in} - T_{fc}\right)e^{\left(-\frac{h_{cw}S_{cw}}{\dot{m}_w c_w}\right)} \tag{11}$$

where h_{cw} and S_{cw} represent the forced convection heat transfer coefficient and the heat transfer surface, respectively.

Substituting $T_{w,out}$ in Eq. (10) by its expression (11) yields:

$$\dot{Q}_{whe} = k_w\left(T_{w,in} - T_{fc}\right) \tag{12}$$

where:

$$k_w = \dot{m}_w c_w\left(1 - e^{\left(-\frac{h_{cw}S_{cw}}{\dot{m}_w c_w}\right)}\right)$$

The solution of the system for differential Eq. (8) is given by:

$$T_{fc}\left(t\right) = T_{fc}^{\infty} + \left(T_{fc}^{\infty} - T_{fc}^{\infty} - C\right)e^{-r_1 t} + Ce^{-r_2 t} \tag{13}$$

where:

$$T_{fc}^{\infty} = T_{amb} + \frac{P_{he}}{h_{nc}S_{nc}} \tag{14}$$

and where:

$$C = \frac{\frac{k_w}{C_{fc}}T_w^0 + \frac{k_w}{C_w}T_{fc}^0 + \frac{h_{nc}S_{nc}}{C_{fc}}T_{amb} - T_{fc}^0 r_2 - T_{fc}^{\infty} r_1}{(r_1 - r_2)} \tag{15}$$

and where:

$$r_1 = -\frac{1}{2}\left(\frac{h_{nc}S_{nc}}{C_{fc}} + \frac{k_w}{C_{fc}} + \frac{k_w}{C_w}\right) + \frac{1}{2}\sqrt{\left(\frac{h_{nc}S_{nc}}{C_{fc}} + \frac{k_w}{C_{fc}} + \frac{k_w}{C_w}\right)^2 - 4\frac{k_w}{C_w}\frac{h_{nc}S_{nc}}{C_{fc}}} \tag{16}$$

$$r_2 = -\frac{1}{2}\left(\frac{h_{nc}S_{nc}}{C_{fc}} + \frac{k_w}{C_{fc}} + \frac{k_w}{C_w}\right) - \frac{1}{2}\sqrt{\left(\frac{h_{nc}S_{nc}}{C_{fc}} + \frac{k_w}{C_{fc}} + \frac{k_w}{C_w}\right)^2 - 4\frac{k_w}{C_w}\frac{h_{nc}S_{nc}}{C_{fc}}} \tag{17}$$

And where $C_{fc} = m_{fc}c_{fc}$ and $C_w = m_w c_w$ are the heat capacity of the PEMFC and of the heating fluid respectively.

Consider that the ambient temperature is lower than T_{fc}^{min} (the minimum prescribed temperature for the fuel cell operation). The role of the warm-up system is to increase T_{fc} up to T_{fc}^{min} by heating the stack. However, if the system starts heating too earlier, a part of the energy is lost into the environment through the natural convection. So in the next section, we propose a simple method that will allow determining the most appropriate time to start heating the stack.

4.2. Time to start heating the fuel cell stack

To minimize the heat transfer between the stack and the environment during the warm-up process, the heating duration must be short and adequate to bring the fuel cell temperature close the T_{fc}^{min}. So, given the time to start the fuel cell $\tilde{t}_{st}$, the shortest heating duration t_{he} is computed using Eq. (13). In practice, we have found that the following approximation can adequately represent the heating duration:

$$t_{he} \approx -\frac{C_{fcw}}{h_{nc}S_{nc}}\ln\left[\frac{h_{nc}S_{nc}\left(T_{fc}^{min} - T_{amb}\right) - P_{he}}{h_{nc}S_{nc}\left(T_{fc}^{0} - T_{amb}\right) - P_{he}}\right] \tag{18}$$

where:

$$C_{fcw} = m_w c_w + m_{fc}c_{fc} \tag{19}$$

So, by taking into account the estimated time to start the fuel cell $\tilde{t}_{st}$, we obtained the expression of the time to start heating the stack $t_{st,he}$ as followed:

$$t_{st,he} \approx \tilde{t}_{st} - t_{he} \tag{20}$$

The total energy used from the batteries by the warm-up system is therefore approximated as follows:

$$U_{he} = \int_{t_{st,he}}^{\tilde{t}_{st}} P_{he}dt = P_{he}\left(t_{\tilde{t}_{st}} - t_{st,he}\right) \tag{21}$$

5. Stack self heating

As the stack temperature reaches the minimum prescribed temperature T_{fc}^{min}, the PEMFC can be started. The efficiency which depends on the cell temperature is low. Increasing the temperature by providing external heat can help to improve this efficiency and avoid ice formation near the freezing temperature. However, this method is inefficient since the electric energy used to accelerate the stack warm-up is no longer available for the vehicle traction. Since the electricity production in the PEMFC is exothermic, the heat from the reaction can be used as a self-heating energy to increase the stack temperature. In this section, we propose a method to determine the optimal level of the fuel cell power production in order to increase quickly the stack temperature and avoid ice formation.

5.1. Optimal current profile

5.1.1. Problem formulation

As the fuel cell temperature reaches T_{fc}^{min}, the PEMFC is started and the warm-up system is stopped. The evolution of the PEMFC temperature depends on the amount of heat provided by the two

heat sources: the mass species heat rate $\dot{Q}_{mst}$ and the reaction heat rate $\dot{Q}_{rh}$. The heat introduced by the reaction depends on the PEMFC efficiency, and it is affected by several operating parameters such as the load current, the cell temperature, the membrane water content, air stoichiometry ratio, the anode and the cathode pressures, etc. The dynamics of the fuel cell average temperature are represented by the following first-order differential equation:

$$m_{fc}c_{fc}\frac{dT_{fc}}{dt} = \dot{Q}_a + \dot{Q}_{rh} - \dot{Q}_{amb} \tag{22}$$

where $\dot{Q}_{amb}$ is represented by Eq. (9); $\dot{Q}_{rh}$ is the reaction heat transfer rate (see Eq. (25)); $\dot{Q}_a$ is the air flow heat transfer rate (see Eq. (23)). The hydrogen heat transfer rate is neglected in this model.

As in the case of forced convection (see Eqs. (10)–(12)), the heat transfer rate between the air and the stack is:

$$\dot{Q}_a = k_a\left(T_{a,in} - T_{fc}\right) \tag{23}$$

where:

$$k_a = \dot{m}_a c_a\left(1 - e^{\left(-\frac{h_a S_a}{\dot{m}_a c_a}\right)}\right) \tag{24}$$

And where $\dot{m}_a$, c_a, h_a, S_a and $T_{a,in}$ represent the air flow rate, the specific heat coefficient of the air, the forced convection heat transfer coefficient of the air, the heat transfer surface between the air and the stack and the inlet air temperature, respectively. The reaction heat rate is represented by [17]:

$$\dot{Q}_{rh} = \left(-\frac{\Delta H_{rh}}{2F} - V_{cell}\right) I_{fc} N \tag{25}$$

where ΔH_{rh}, F, V_{cell}, I_{fc} and N represent the enthalpy of the formation [18], the Faraday constant, the cell voltage as represented in Ref. [19], the stack output current and the number of cells.

The cell voltage is given by:

$$V_{cell} = V_{ocv} - V_{ohm} - V_{act} - V_{con} \tag{26}$$

where V_{ocv}, V_{ohm}, V_{act} and V_{con} represent the open-circuit voltage or Nernst voltage, the ohmic loss, the activation loss and the concentration loss.

Linearizing Eq. (22) yields:

$$\dot{T}_{fc} = AT_{fc} + Bu\left(t\right) \tag{27}$$

where:

$$A = -\frac{k_a + h_{cn}S_{cn}}{m_{fc}c_{fc}} \tag{28}$$

and where:

$$B = \frac{1}{m_{fc}c_{fc}} \tag{29}$$

and where:

$$u\left(t\right) = \dot{Q}_{rh} + h_{cn}S_{cn}T_{amb} + k_a T_{a,in} \tag{30}$$

Given the temperature dynamics represented by Eq. (27), the objective is to find the current profile I_{fc} (see Eqs. (25) and (30)) that will quickly increase the stack temperature from T_{fc}^{min} to T_{fc}^{max}. This current must not exceed the maximum prescribed current $I_{fc}^{max} > 0$.

So we formulate a minimum time optimization problem as follows: find the optimal heat rate $u(t)$ that minimizes the cost function represented by Eq. (31) under the constraint of the stack temperature dynamics represented by Eq. (27).

$$J = \int_{\tilde{t}_{st}}^{t_{fc,min}} dt \tag{31}$$

where $t_{fc,min}$ represents the minimum time it takes for the fuel cell temperature to reach the maximum prescribed temperature T_{fc}^{max}. $\tilde{t}_{st}$ is obtained by Eq. (7).

5.1.2. Solving the time optimal problem

The Hamiltonian of the system is represented by [16]:

$$\mathcal{H}\left(T_{fc}, \lambda, u, t\right) = 1 + \lambda\left(t\right)\left(AT_{fc}\left(t\right) + Bu\left(t\right)\right) \tag{32}$$

where λ represents the system costate variable which differential equation is given by:

$$-\dot{\lambda}\left(t\right) = \frac{\partial\mathcal{H}\left(T_{fc}, \lambda, u, t\right)}{\partial T_{fc}} \tag{33}$$

Differentiating Eq. (32) and using Eq. (33) yields:

$$-\dot{\lambda}\left(t\right) = A\lambda\left(t\right) \tag{34}$$

Hence, the solution of this differential equation is given by:

$$\lambda\left(t\right) = \lambda\left(t_{fc,min}\right)e^{-A\left(t_{fc,min}-t\right)} \tag{35}$$

Since $t_{fc,min}$ is free, $dt_{fc,min} \neq 0$. The transversality condition becomes:

$$\mathcal{H}\left(T_{fc}, \lambda, u, t_{fc,min}\right) = 0 \tag{36}$$

This equation is equivalent to:

$$1 + \lambda\left(t_{fc,min}\right)\left(AT_{fc}\left(t_{fc,min}\right) + Bu\left(t_{fc,min}\right)\right) = 0 \tag{37}$$

Since we would like to have $T_{fc}(t_{fc,min}) = T_{fc}^{max}$, the costate value $\lambda(t_{fc,min})$ is computed as follows:

$$\lambda\left(t_{fc,min}\right) = -\frac{1}{AT_{fc}^{max} + Bu\left(t_{fc,min}\right)} \tag{38}$$

If a minimum time optimal control u^* exists, then the Pontryagin minimum principle states that [16]:

$$\mathcal{H}\left(T_{fc}^*, \lambda^*, u^*, t\right) \leq \mathcal{H}\left(T_{fc}^*, \lambda^*, u, t\right) \tag{39}$$

where T_{fc}^*, λ^* and u^* represent the optimal fuel cell temperature profile, the optimal costate profile and the optimal heat rate, respectively.

Using the Hamiltonian Eq. (32), the expression (39) becomes:

$$\lambda^*\left(t\right)Bu^*\left(t\right) \leq \lambda^*\left(t\right)Bu\left(t\right) \tag{40}$$

Hence, the optimal heat rate $u^*(t)$ is obtained by the following equation [16]:

$$u^*(t) = -\mathrm{sgn}(B\lambda(t))u^{max} \tag{41}$$

where:

$$\mathrm{sgn}(B\lambda(t)) = \begin{cases} 1, & \text{if } B\lambda(t)>0 \\ \text{indeterminate}, & \text{if } B\lambda(t) = 0 \\ -1, & \text{if } B\lambda(t) < 0 \end{cases} \quad (42)$$

and where $u^{\max}$ is the maximum heat rate that can be applied to the stack.

Eq. (42) shows that the optimal heat rate will always take the extremum values of u. Hence $u^*(t)$ will take only two values:

- $u^*(t) = u^{\max}$ if $(B\lambda(t))$ is negative;
- $u^*(t) = -u^{\max}$ if $(B\lambda(t))$ is positive.

In the case of $\lambda(t) = 0$, there is a singularity. Fortunately, this case will not occur if $u^{\max}$ is very high as demonstrated below. Assume that $u^*(t_{\mathrm{fc,min}}) = u^{\max}$; the final value of the optimal costate is given by:

$$\lambda\left(t_{\mathrm{fc,min}}\right) = -\frac{1}{AT_{\mathrm{fc}}^{\max} + Bu^{\max}} \quad (43)$$

So, the costate profile which is derived from Eq. (35) becomes:

$$\lambda(t) = -\frac{1}{AT_{\mathrm{f\,c}}^{\max} + Bu^{\max}} e^{-A\left(t_{\mathrm{f\ c,min}} - t\right)} \quad (44)$$

If there is enough heating power to warm-up the stack then:

$$u^{\max} > -\frac{A}{B} T_{\mathrm{fc}}^{\max} \quad (45)$$

In this case, $\lambda(t) < 0$ which confirms that $u^*(t_{\mathrm{fc,min}}) = u^{\max}$. In addition, $\lambda(t)$ cannot be equal to 0. Clearly, there is no singularity with this control law under the condition (45). The minimum time optimal solution is therefore to apply $u^{\max}$. The maximum reaction heat rate $\dot{Q}_{\mathrm{rh}}^{\max}$ which corresponds to $u^{\max}$ can be computed using Eq. (30). Then, the optimal current profile is obtained by Eq. (25).

6. High temperature regulation

When the fuel cell temperature reaches the maximum prescribed temperature $T_{\mathrm{fc}}^{\max}$, it should be regulated in order to avoid overheating the stack. The high temperature regulation has been extensively studied in the literature. In this paper, a simple PID regulator was used to maintain the fuel cell temperature close to $T_{\mathrm{fc}}^{\max}$.

Fig. 3 illustrates the different energies involved in the PEMFC during the course of a driving cycle. During the first stage (pre-startup or warm-up phase), external heating power is provided to the stack. During this pre-startup phase there is no power production from the PEMFC. As the stack temperature is rising, this external power is removed and the fuel cell is started to begin producing heat (blue color zone) and electric power (shaded green zone). However, the low efficiency at the beginning of its operation leads to more heat generation than electric production (startup stage). When the temperature reaches the maximum prescribed, the efficiency is high which reduces the proportion of the heat versus the electricity.

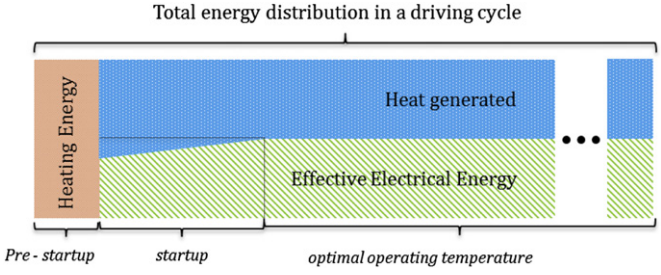

Fig. 3. Energy distribution during a driving cycle.

7. Experimental validation and discussions

7.1. Experimental goal

The experiments aim at validating the following methods:

- the estimation of the Energy Management System of the time to start the fuel cell;
- the estimation of the time to start heating the stack;
- the fuel cell thermal model during the stack self-heating stage;
- the time minimal solution approach proposed in this paper.

7.2. Experimental setup

A specific test bench was built with a small commercial 500 W PEMFC which picture is shown in Fig. 4. The experimental parameters are presented in Table 1. The complete setup is represented in Fig. 5. In this figure, we have an air supply circuit, a hydrogen supply circuit operating in dead-end conditions and a fluid cooling circuit.

The air supply circuit includes a compressor, a mass flow meter, an air pressure sensor, and a solenoid valve. To control the air relative humidity and the inlet air temperature, we use a humidifier and a thermostatic bath. The hydrogen circuit includes a hydrogen tank a solenoid which is periodically opened to purge water on the cathode side of the fuel cell stack.

The fluid cooling circuit includes a thermostatic bath (see Fig. 6) which is controlled using a personal computer. An electronic variable load, controlled by the computer, is connected to the output of

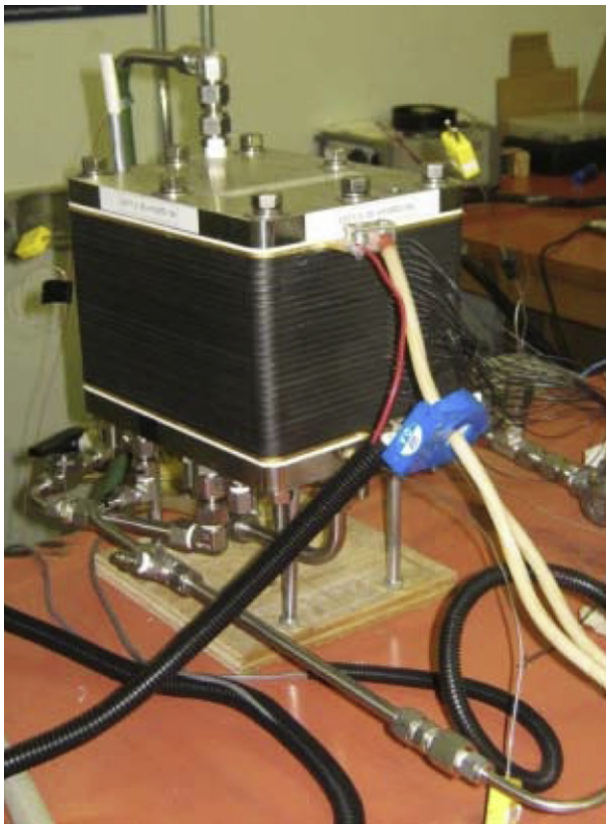

Fig. 4. Hyteon 500 W PEMFC system.

Table 1
Experimental parameters.

Parameters		Values
Stack	N	23 (Cell)
	m_{fc}	12 kg
	c_{fc}	770 (J kg^{-1} K^{-1})
Natural convection	h_{nc}	5 (W K^{-1} m^{-2})
	S_{nc}	0.24 (m^2)
Air forced convention	c_a	1.0 (kJ kg^{-1} K^{-1})
	h_a	90 (W K^{-1} m^{-2})
	S_a	0.4968 (m^2)
	$\dot{m}_a$	$3.57 \times 10^{-7}\lambda_a I_{fc} N$ (kg s^{-1})
	λ_a	2.4
Water forced convection	c_w	4200 (kJ kg^{-1} K^{-1})
	m_w	2 (kg)
	h_{cw}	34 (W K^{-1} m^{-2})
	S_{cw}	0.5962 (m^2)
	$\dot{m}_w$	0.055 (kg s^{-1})

the fuel cell stack. This variable load is used to emulate the FC-PHEV power demand during the experiments.

The computer hosts all the Labview programs relative to the methods described throughout this paper. The main user interface is represented in Fig. 7. The hardware for the signal acquisition and the system control is built with the National Instrument devices.

Our setup was unable to run the experiments with low temperature conditions. So we decide to perform the tests with a temperature range of [293.15 K, 323.15 K]. This range is sufficient to test the proposed methods and to validate the overall PEMFC temperature management strategy.

7.3. Test scenario

7.3.1. Driving cycle and FC-PHEV power demand

A driving cycle obtained when an experimental electric vehicle was moving on the campus of "Université du Québec à Trois-Rivières" is used for the test and the validation of the proposed methods. Knowing the vehicle parameters and the driving cycle, we computed the power demand P_m. A down scale coefficient is applied to the calculated P_m in order to match the fuel cell power production which maximum value is set to 500 W. This power demand is represented in Fig. 8.

7.3.2. Energy management system (EMS) parameters

The battery energy is represented by the State-Of-Charge (SOC) which is the ratio between E_b and E_b^0. At the beginning of the experiment, the State-Of-Charge (SOC) of the batteries is 86.8%. The minimum SOC to start the PEMFC is set to 85%.

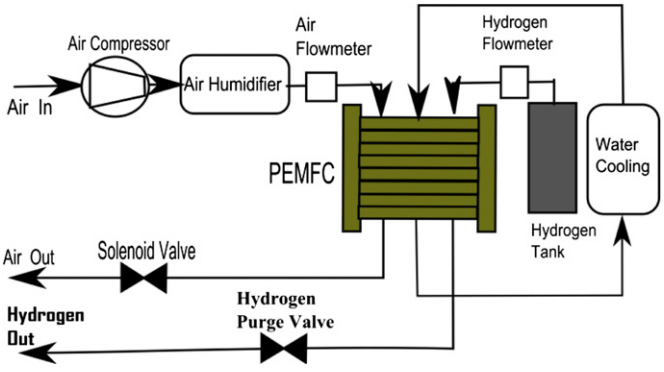

Fig. 5. Experimental PEMFC test bench setup.

Fig. 6. NESLAB RTE thermostatic bath circulator.

As the experiment is running, the EMS must estimate in real-time the time $\tilde{t}_{st}$ for the SOC to reach 85%, using only the past data from P_m and Eq. (7).

7.3.3. PEMFC thermal controller parameters

The fuel cell stack has no thermal insulation and the ambient temperature measured is 297 K. To test the different stages involved in the fuel cell cold start problem (warming stage, self-heating stage and high temperature stage), we select the following operating conditions which can be easily managed by our test bench system:

- At the beginning ($t = 0$), the temperature of the stack T_{fc}^0 is the same as the ambient temperature ($T_{amb} = 297.15$ K).
- The PEMFC operating range is set to [303.15 K, 323.15 K]. The minimum operating temperature $T_{fc}^{min} = 303.15$ K is greater than the ambient temperature in order to allow the warm-up system (the thermostatic bath) to heat the stack and increase T_{fc} from T_{fc}^0 to T_{fc}^{min}. This process will emulate the warming-up stage of the cold start strategy.
- The maximum power for the warm-up system is 700 W. The cooling fluid is the water circulating in a closed-loop circuit.
- From 303.15 K to $T_{fc}^{max} = 323.15$ K, the fuel cell is in the self-heating phase where the reaction heat is used to increase quickly the temperature of the stack.
- As the temperature reaches T_{fc}^{max}, the process regulation is started.

7.4. Experimental and simulation results

In this section, we present a comparative study between the simulation and the experimental results when the test scenario described above is executed on our test bench.

Fig. 7. User interface for the monitoring and the control of the PEMFC system.

7.4.1. Validation of the time to start the PEMFC

Using the power demand represented in Fig. 8, the time to start the fuel cell is estimated based on the history of P_m. Fig. 9 shows the real-time estimation of $\tilde{t}_{st}$ which is obtained by using Eq. (7). For comparison purpose, we determined off-line the time for the SOC to reach 85% by considering all the time sequence of the power demand. This evaluation ($t_{st} = 1000\ s$) is represented by the dash line in Fig. 9.

One can observe in Fig. 9 that at the beginning, the estimation $\tilde{t}_{st}$ was too far from the value of t_{st}. As the experiment is running, and the number of past data of P_m is increasing, the estimation error becomes small, despite the big variation of the power demand signal. In Fig. 10, the fuel cell starts the power production at $t = 1029\ s$ which is greater than t_{st}. This small lag is due to: (i) the stack temperature sensor position which measures a local temperature within the stack and (ii) the valves activation delays (anode and cathode valves). Nevertheless, when the fuel cell was started, the SOC decreasing rate is significantly reduced. This result suggests that the proposed method can be used to perform a fairly good real-time estimation of the time to start running the PEMFC.

7.4.2. Estimation of the time to start heating the stack

Given $\tilde{t}_{st}$, the fuel cell temperature controller must determine the time to start the warm-up system $t_{st,he}$ based on the different heat transfer characteristics, the ambient temperature T_{amb}, the fuel cell minimum T_{fc}^{min}, the heating duration t_{he}, the time to start the fuel cell $\tilde{t}_{st}$ and the heating power that can be provided by the

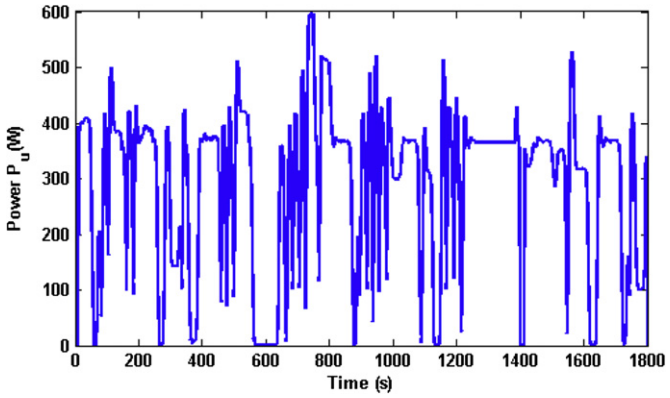

Fig. 8. FC-PHEV power demand based on a down scaled experimental driving cycle.

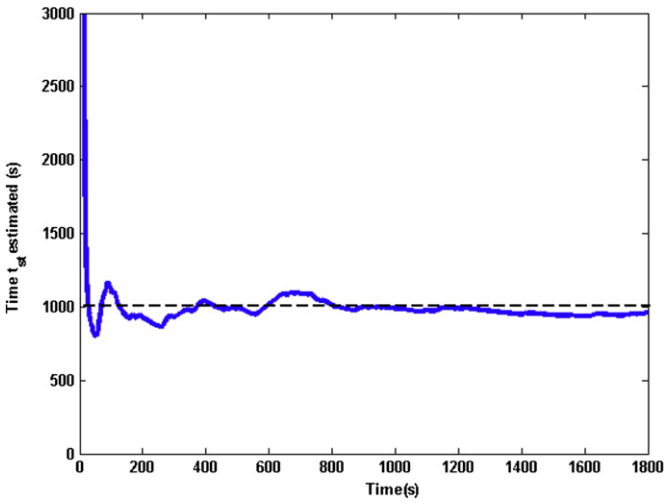

Fig. 9. Real-time estimation of t_{st}.

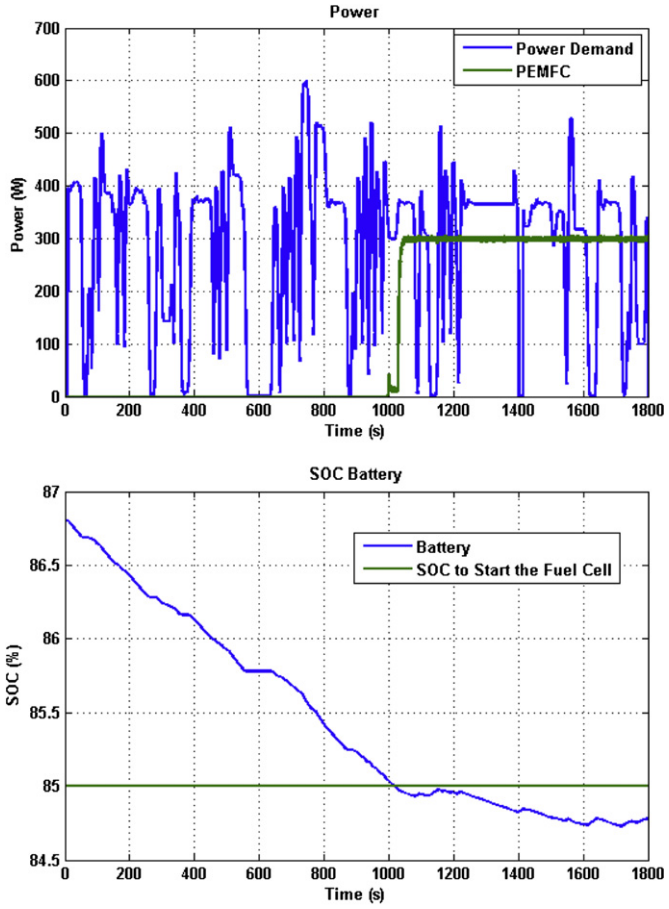

Fig. 10. Energy flow during the experiment.

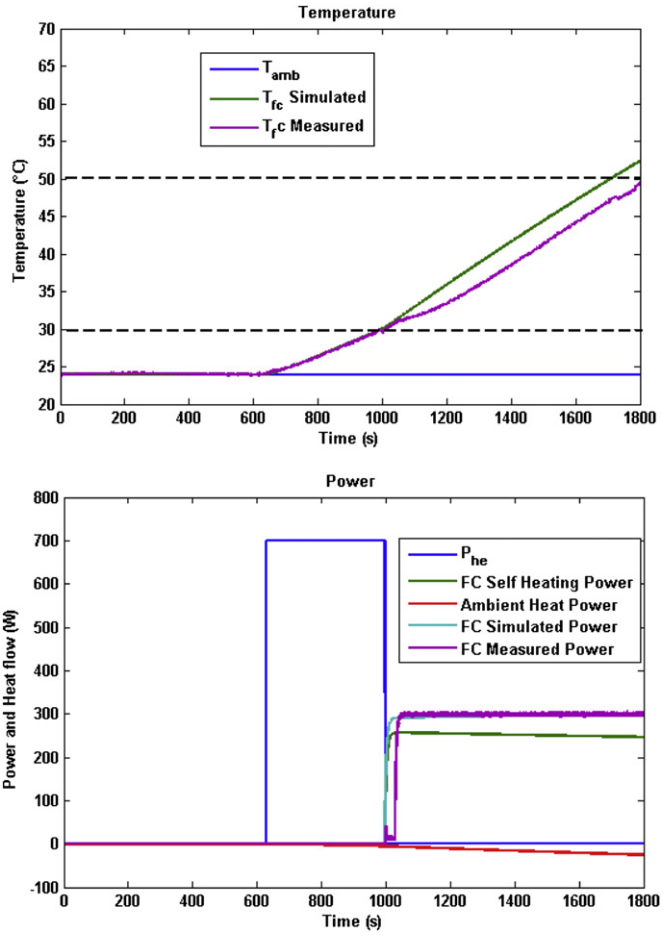

Fig. 11. Experimental result.

warm-up system P_{he}. As we said before, $T_{fc}^{0} = T_{amb}$ at the beginning of the experiments.

Using Eq. (18), the time to start heating is estimated to 628 s as shown in the lower graph of Fig. 11. If this estimation is good, the stack temperature should be close to the minimum temperature T_{fc}^{min} at $t = \tilde{t}_{st}$ so that the fuel cell can start on time.

In Fig. 11 (first graph), one can observe that the fuel cell temperature is close to 30 °C which corresponds to $T_{fc}^{min} = 303.15$ K at $t = 1029$ s. Although the presence of this lag of 29 s (which represents only 2.9% of t_{st} value), this experimental result suggests that the method to estimate the time to start heating the fuel cell is good enough.

7.4.3. Fuel cell thermal model during the stack self heating stage

As the fuel cell temperature reaches T_{fc}^{min}, the fuel cell is automatically started (see the pink curve of the second graph in Fig. 11). The self produced heat by the stack is shown in the second graph, the green curve, whilst the electric power produced by the fuel cell is represented in the same graph, the pink curve. The stack temperature rises from 24 °C (297.15 K) to 50 °C($T_{fc}^{max} = 323.15$ K). During the self-heating stage, the comparison between the simulated fuel cell temperature and the measured temperature indicates that both curves have a similar trend. However, the experimental temperature is shifted down by 7% because of:

- The fuel cell nonlinear temperature behavior that is not well included into the developed lumped model (see Eq. (22)).
- The position of the temperature sensor in the stack. A more interesting way to capture the fuel cell average temperature would be to use several sensors at several positions within the stack.

For automotive application with a serial topology, this level of mismatch between the lumped model and the experimental one is acceptable since there is no need for the fuel cell to precisely track the power demand.

Since the maximum heating power was used by the warm-up system (see Fig. 11, the second graph, the blue curve), the stack heating duration is the shortest one. Otherwise, a more powerful heating system should be used.

7.4.4. Global strategy simulation

The simulation aims at: (i) providing the stack thermal behavior when the starting temperature belongs to the sub-freezing range; (ii) comparing the energy used to warm-up the stack during a given trip. We consider an extended version of the vehicle power demand used for the experimentation and shown in Fig. 8. The extension power demand profile, obtained by concatenating several times the experimental one, has a duration of 5000 s. In addition, we suppose that:

- the initial stack temperature is −20 °C (253.15 K);
- the stack maximum operating temperature is $T_{fc}^{max} = 60$ °C (233.15 K);
- the minimum operating temperature is $T_{fc}^{min} = 5$ °C.

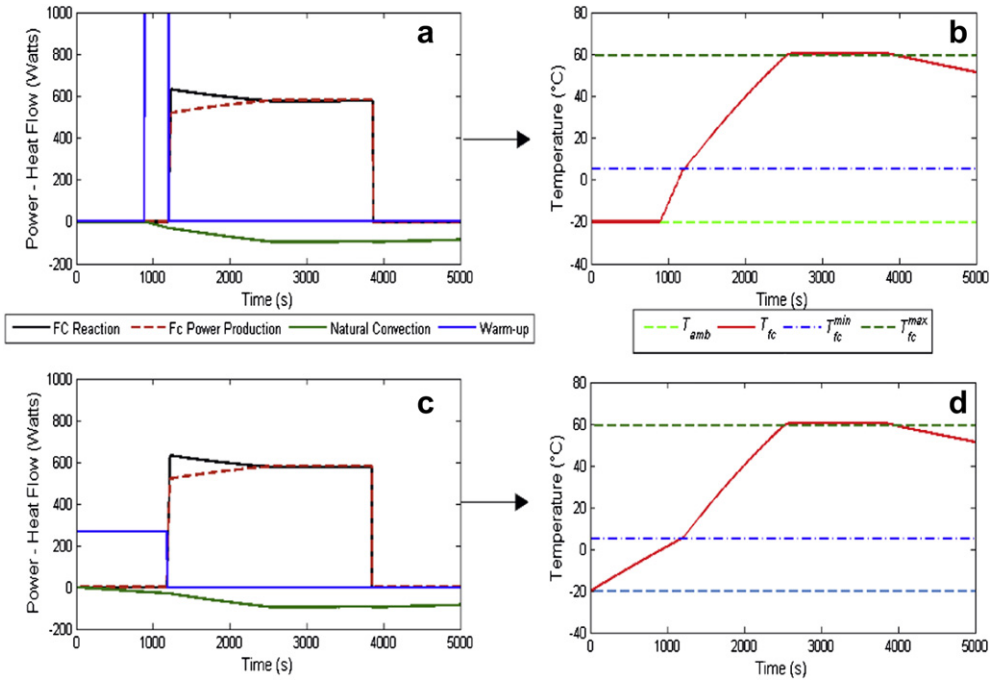

Fig. 12. Simulations results.

During the warm-up phase (when the stack temperature belongs to [−20 °C, 5 °C]), we used the same external warm-up system characteristics as the experimentation one. However, in order to show the heat losses through the natural convection, we analyze two scenarios. In the first one (called scenario 1), we suppose that the selected warm-up system operates at its maximum heating power (700 W). This scenario corresponds to the heating strategy proposed in this paper. In the second scenario (called scenario 2), we consider that the warm-up system starts heating with a constant heating power which is less than the maximum one and which will let the stack temperature to reach T_{fc}^{min} at the prescribed time to start the fuel cell ($\tilde{t}_{st}$). During the self-heating phase, the proposed time optimal strategy is used.

Fig. 12 shows the simulation result. The graphs (a) and (b) are related to scenario 1 whereas the graphs (c) and (d) are related to scenario 2. With both scenarios, the fuel cell temperature reaches the T_{fc}^{min} at the prescribed time $\tilde{t}_{st}$. However, during the warm-up phase, the heat losses due to natural convection with scenario 1 (green curve in the graph (a)) is less than convection losses with scenario 2 (green curve in the graph (c)). The energy used by the warm-up system with scenario 1 and with scenario 2 are 0.304 MJ and 0.317 MJ, respectively. These results indicate that the proposed heating strategy in the warm-up phase is effective.

8. Conclusion

A global strategy for a PEMFC cold startup is investigated through a theoretical analysis and an experimental validation on a laboratory test bench. This strategy aims at providing an efficient method to manage a PEMFC thermal behavior within the framework of a Fuel Cell Plug-in Hybrid Vehicle (FC-PHEV) with a serial topology. The Energy Management System (EMS) based on a supervisory architecture is proposed, implemented and validated. This system estimates in advance and in real-time, the time to start the fuel cell based on the time for the battery energy to reach a minimum prescribed energy. Given this estimation and the amount of additional energy required, the fuel cell temperature management strategy computes the most appropriate time to start heating the stack in order to reduce the heat loss through the natural convection. To quickly increase the temperature when the fuel cell is started, we propose the use of the reaction heat as a heat power source through a time optimal control law. The experimental results have shown that the proposed approach is efficient and can be implemented in real-time on FC-PHEVs.

Acknowledgment

This work was supported by the Bureau de l'efficacité énergétique, Ministère des Ressources naturelles et de la Faune du Québec, the Natural Science and Engineering Research Council of Canada and the LTE Hydro-Quebec.

References

[1] S.J. Moura, J.B. Siegel, D.J. Siegel, H.K. Fathy, A.G. Stefanopoulou, Vehicle Power and Propulsion Conference (VPPC) (2010) 1–6.
[2] Y. Haseli, G. Naterer, I. Dincer, International Journal of Hydrogen Energy 33 (2008) 1788–1796.
[3] D. Feroldi, M. Serra, J. Riera, IEEE Transactions on Vehicular Technology 58 (2009) 4720–4729.
[4] Z. Yu, D. Zinger, A. Bose, Journal of Power Sources 196 (2011) 2351–2359.
[5] S. Wirasingha, A. Emadi, IEEE Transactions on Vehicular Technology 60 (2011) 111–122.
[6] A. Stefanopoulou, K.-W. Suh, Control Engineering Practice 15 (2007) 277–289.
[7] A.A. Pesaran, G.Heon Kim, J.D. Gonder, National Renewable Energy Laboratory (2005).
[8] A. Faghri, Z. Guo, International Journal of Heat and Mass Transfer 48 (2005) 3891–3920.
[9] Q. Yan, H. Toghiani, Y.-W. Lee, K. Liang, H. Causey, Journal of Power Sources 160 (2006) 1242–1250.
[10] R. Alink, D. Gerteisen, M. Oszcipok, Journal of Power Sources 182 (2008) 175–187.
[11] M. Sundaresan, R.M. Moore, Journal of Power Sources 145 (2005) 534–545.
[12] M. Sundaresan, Ph.D. dissertation, Davis, University of California, 2004.
[13] S. Sun, H. Yu, J. Hou, Z. Shao, B. Yi, P. Ming, Z. Hou, Journal of Power Sources 177 (2008) 137–141.
[14] C. Ernst, A. Hackbarth, R. Madlener, B. Lunz, D. Sauer, E. Lutz, FCN Working Paper No. 14 (2010).
[15] X. Li, J. Li, L. Xu, M. Ouyang, Vehicle Power and Propulsion Conference, VPPC '09 (2009) 1749–1754.

[16] F. Lewis, V. Syrmos, Optimal Control, John Willey & Son, New York, 2005.
[17] K.P. Adzakpa, et al., Journal of Power Sources 179 (2008) 164–176.
[18] A. Dicks, J. Larminie, Fuel Cell Systems Explained, second ed. John Wiley & Sons Ltd, 2003.
[19] R.F. Mann, J.C. Amphlett, M.A.I. Hooper, H.M. Jensen, B.A. Peppley, P.R. Roberge, Journal of Power Sources 86 (2000) 173–180.
[20] F.P. Incropera, D.P. DeWitt, Fundamentals of Heat and Mass Transfer, J. Wiley, 2002.
[21] L. Mao, C.-Y. Wang, Journal of the Electrochemical Society 154 (2007) B139.
[22] F. Jiang, C.-Y. Wang, K.S. Chen, Journal of the Electrochemical Society 157 (2010) B342.
[23] E.L. Thompson, J. Jorne, H.A. Gasteiger, Electrochemical Society (2007) 565–576.
[24] K. Haraldsson, K. Wipke, Journal of Power Sources 126 (2004) 88–97.
[25] Y. Ferng, International Journal of Hydrogen Energy 29 (2004) 381–391.

Nomenclature

Alphabets
c: specific heat
C: specific heat capacity
E: energy
F: Faraday constant
ΔH: enthalpy of formation
h: convection heat transfer coefficient
I: electric current
m: thermal mass
$\dot{m}$: mass flow rate
P: power
$\dot{Q}$: rate of the heat
S: effective heat transfer surface
t: time
T: temperature
V: voltage

Greek symbols
η: efficiency
λ_a: stoichiometric air ratio

Superscripts and subscripts
a: air
act: activation
amb: ambient
b: battery pack
cell: cell of the stack
con: concentration
cw: water forced convection
fc: fuel cell
he: warm-up system heater element
in: inlet
m: mechanic
max: maximum
min: minimum
mst: mass species transportation
nc: natural convection
ohm: Ohmic
out: outlet
ocv: open circuit voltage
rh: hydrogen with oxygen reaction
st: start time
td: road trip duration
tr: traction
u: vehicle user
w: fluid
whe: fluid heat exchanger